Published in final edited form as:

Cancer Res. 2022 August 16; 82(16): 2848–2859. doi:10.1158/0008-5472.CAN-21-3552.

The prostate cancer androgen receptor cistrome in African American men associates with upregulation of lipid metabolism and immune response

Jacob E. Berchuck[1,2,3,*], **Elio Adib**[1,2,*], **Sarah Abou Alaiwi**[2,3,*], **Amit K. Dash**[4,*], **Jin Na Shin**[4], **Dallin Lowder**[4], **Collin McColl**[4], **Patricia Castro**[5,6], **Ryan Carelli**[7], **Elisa Benedetti**[7], **Jenny Deng**[4], **Matthew Robertson**[6], **Sylvan C. Baca**[1,2], **Connor Bell**[1,2], **Heather M. McClure**[1,2], **Talal E. Zarif**[1,2], **Matthew P. Davidsohn**[1,2], **Gitanjali Lakshminarayanan**[1,2], **Kinza Rizwan**[4], **Darlene Skapura**[4], **Sandra L. Grimm**[6], **Christel M. Davis**[8], **Erik A. Ehli**[8], **Kaitlin M. Kelleher**[1], **Ji-Heui Seo**[1,2], **Nicholas Mitsiades**[4,6,9], **Cristian Coarfa**[6,9], **Mark M. Pomerantz**[1,2], **Massimo Loda**[7], **Michael Ittmann**[5,6], **Matthew L. Freedman**[1,2,**], **Salma Kaochar**[4,6,9,**]

[1]Department of Medical Oncology, Dana-Farber Cancer Institute, Boston, MA, USA

[2]Center for Functional Cancer Epigenetics, Dana-Farber Cancer Institute, Boston, MA, USA

[3]Department of Medicine, Brigham and Women's Hospital, Boston, MA, USA

[4]Department of Medicine, Baylor College of Medicine, Houston, TX, USA

[5]Department of Pathology, Baylor College of Medicine, Houston, TX, USA

[6]Dan L Duncan Cancer Center, Baylor College of Medicine, Houston, TX, USA

[7]Avera Institute for Human Genetics, Sioux Falls, SD USA 57108

[8]Department of Pathology and Laboratory Medicine, Weill Cornell Medicine, New York, New York.

[9]Department of Molecular and Cellular Biology, Baylor College of Medicine, Houston, TX, USA

Abstract

African American (AA) men are more likely to be diagnosed with and die from prostate cancer (PCa) than European American (EA) men. Despite the central role of the androgen receptor (AR) transcription factor in PCa, little is known about the contribution of epigenetics to observed racial disparities. We performed AR ChIP-seq on primary prostate tumors from AA and EA men, finding

Corresponding Authors: Matthew L. Freedman, 450 Brookline Ave, Smith 1058, Boston, MA, 02215, 617-582-8598, freedman@broadinstitute.org, Salma Kaochar, 1 Baylor Plaza, New Alkek ABBR R404, Houston, Texas, 77030, 713-798-1112, kaochar@bcm.edu.

*equal contribution (J.E.B., E.A., S.A.A., A.K.D.)

**equal contribution (M.L.F., S.K.)

Author Contributions: J.E.B., E.A., S.A.A., A.K.D., J.N.S., D.L., R.C., E.B., S.C.B., D.S., M.M.P., M.L., M.L.F., S.K. conceived and designed experiments. J.E.B., E.A., S.A.A., A.K.D., J.N.S., D.L., C.M., R.C., E.B., J.D., C.B., H.M.M., T.E.Z, J.H.S., K.R., D.S., C.M.D., E.A.E. performed experiments. J.E.B., E.A., S.A.A., A.K.D., J.N.S., D.L., C.M., R.C., E.B., J.D., M.R., S.C.B., J.H.S., K.R., D.S., S.L.G., C.M.D., E.A.E., C.C., M.M.P., M.L., M.L.F., S.K. analyzed and interpreted data. P.C., N.M., M.M.P., M.I., S.K. contributed patient samples. J.E.B., E.A., S.A.A., P.C., C.B., H.M.M., K.M.K., N.M., M.M.P., M.I. collected patient data and samples. J.E.B., E.A., S.A.A., A.K.D., P.C., J.N.S., D.L., C.M., J.D., S.C.B., J.H.S., K.R., D.S., C.M.D., E.A.E., N.M., M.M.P., M.L., M.I., M.L.F., S.K. provided guidance and scientific input. J.E.B., E.A., S.A.A., M.L.F., S.K. drafted the manuscript. All authors read and approved the final manuscript.

Conflict-of-Interest Statement: No authors report conflicts of interest relevant to the content in this manuscript.

that sites with greater AR binding intensity in AA relative to EA PCa are enriched for lipid metabolism and immune response genes. Integration with transcriptomic and metabolomic data demonstrated coinciding upregulation of lipid metabolism gene expression and increased lipid levels in AA PCa. In a metastatic prostate cancer cohort, upregulated lipid metabolism associated with poor prognosis. These findings offer the first insights into ancestry-specific differences in the PCa AR cistrome. The data suggest a model whereby increased androgen signaling may contribute to higher levels of lipid metabolism, immune response, and cytokine signaling in AA prostate tumors. Given the association of upregulated lipogenesis with PCa progression, our study provides a plausible biological explanation for the higher incidence and aggressiveness of PCa observed in AA men.

INTRODUCTION

African American (AA) men are more likely to be diagnosed with prostate cancer (PCa), to be diagnosed at a younger age, to have more aggressive disease, and to die from PCa compared with European American (EA) men.(1,2) While socioeconomic and psychosocial factors contribute, a growing body of literature also supports biological differences underlying these disparities, including ancestry-specific genetic risk and somatic variants, RNA expression, tumor microenvironment, and androgen levels between AA and EA men.(3–7) Comparatively less is known about the role of epigenetics.

Several studies suggest that aberrant DNA methylation, a repressive epigenetic mark, may contribute to PCa aggressiveness in AA men.(8–10) Transcription factors, proteins that bind specific DNA sequences to dynamically regulate gene transcription, are strongly implicated in PCa development.(11–14) We previously demonstrated that the androgen receptor (AR) cistrome is extensively reprogrammed in PCa tumorigenesis and disease progression.(11,12) These findings provided important insights into events that drive normal prostate epithelium to transform into PCa and established epigenetic reprogramming of the AR cistrome as central to prostate tumorigenesis. These data, however, were generated exclusively in samples from EA men. How or if the PCa AR cistrome differs in AA men and whether this contributes to observed racial disparities is not known.

In this study, we present the first description of the AR cistrome in primary PCa from AA men. Our data suggest that differential AR binding in AA and EA PCa may contribute to distinct transcriptional programs, including biological processes known to be dysregulated in prostate tumors in AA men, such as lipid metabolism, immune response, and cytokine signaling.

METHODS

Tissue cohort

Fresh-frozen radical prostatectomy specimens were selected from the Dan L Duncan Comprehensive Cancer Center Human Tissue Acquisition and Pathology Core at Baylor College of Medicine and the Dana-Farber Cancer Institute Gelb Center biobank. A genitourinary pathologist reviewed slides stained with hematoxylin and eosin from each

case and isolated areas enriched for prostate tumor tissue (≥ 50% tumor cellularity) or normal prostate epithelium. 23 subjects were selected for ChIP-seq analysis. Informed consent was obtained from all subjects whose samples were included in the study. This study was approved by the Baylor College of Medicine and the Dana-Farber Cancer Institutional Review Boards.

ChIP-seq data generation and analysis

Using a 2 mm^2 core needle, one core was extracted from frozen RP tissue blocks in the areas marked on the corresponding slide. Frozen cores were pulverized using the Covaris CryoPrep system. The tissue was then fixed using 2 mM disuccinimidyl glutarate (DSG) for 10 minutes followed by 1% formaldehyde buffer for 10 minutes and quenched with glycine. Chromatin was sheared to 300–500 bp using the Covaris E220 ultrasonicator. The resulting chromatin was incubated overnight with 5μg of antibody to AR (RB Anti-AR PAb, spring bioscience, REF: E2724, REF: 05300886001, LOT: 170118LVA) bound to protein A and protein G beads (Life Technologies). 5% of the sample was not exposed to antibody and used as control. The samples were then de-crosslinked, treated with RNase and proteinase K, and DNA was extracted (Qiagen). DNA sequencing libraries were prepared using the ThruPLEX-FD Prep Kit (Rubicon Genomics). Libraries were sequenced on an Illumina HiSeq 4000 to generate 150-bp paired-end reads (Novogene).

ChIP-seq reads were aligned to the human genome build hg19 using the Burrows-Wheeler Aligner (BWA) version 0.7.15.(15) Non-uniquely mapped/redundant reads were discarded. MACS v2.1.1.20140616 was used for ChIP-seq peak calling (q-value < 0.01) and for the generation of the BigWig and BED files.(16) ChIP-seq data quality was evaluated by a variety of measures, including total peak number, FRiP (fraction of reads in peak) score, number of high-confidence peaks, and percent of peak overlap with DHS peaks derived from the ENCODE project. ChIP-seq peaks were assessed for overlap with gene features and CpG islands using annotatr.(17) IGV was used to visualize normalized ChIP-seq read counts at specific genomic loci.(18)

Heatmap clustering, principal component analysis, and identification of subgroup-specific binding sites were performed using Mapmaker (https://bitbucket.org/cfce/mapmaker), a ChIP-seq analysis pipeline implemented with Snakemake.(19) Read counts for each peak were normalized to the total number of mapped reads for each sample. Quantile normalization was applied to this matrix of normalized read counts. Using DESeq2,(20) tumor-specific peaks (T-ARBS) and normal tissue-specific peaks (N-ARBS) were identified at the indicated FDR-adjusted p-value and log2 fold-change cutoffs (p-adjusted < 0.01, log2 fold-change >1) in the AA prostate samples. The same DESeq2 comparison was applied to compare AA and EA prostate tumors (p-adjusted < 0.01, log2 fold-change >1).

Unsupervised hierarchical clustering was performed based on Spearman correlation between samples. Principal component analysis was performed using the prcomp R function. Enriched *de novo* motifs in differential peaks were detected using HOMER version 4.11.(21) The top non-redundant motifs were ranked by adjusted p-value. The GREAT tool was used to assess for enrichment of and MSigDB perturbation annotations among genes near differential ChIP-seq peaks, assigning each peak to the nearest gene within 500kb.

(22) CISTROME-GO(23) was used to assess the gene-level regulatory potential scores and enrichment of KEGG pathways in AA tumor specific ARBS (compared to EA tumors). All differential peaks identified by DESeq2 were used as input (p-adjusted < 0.01, log2 fold-change >1). A half-decay distance of 10.0 kb was set. Single-sample gene set enrichment analysis (ssGSEA)(24) was applied to the quantile normalized matrix of AR ChIP-seq read counts to compute Hallmark (h) and KEGG (c2.cp.kegg) gene set enrichment in each individual AR ChIP-seq sample. Pathway-level z-scores were calculated and used for heatmap plotting.

RNA-seq data generation and analysis

Tissue samples were obtained from the Human Tissue Acquisition and Pathology Core of the Dan L. Duncan Comprehensive Cancer Center at Baylor College of Medicine and were collected from fresh radical prostatectomy specimens after obtaining informed consent under an Institutional Review Board approved protocol. Cancer samples contained a minimum of 70% cancer and benign tissues were free of cancer on pathological examination. RNAs were extracted using Qiagen DNA/RNA Mini kit according to manufacturer's instruction. The isolated total RNA was assessed for quantity and degradation on an RNA 6000 Nano chip ran on a 2100 BioAnalyzer (Agilent; Santa Clara, CA). RNAs with RIN number ≥ 7 were chosen for RNA-seq analysis. Sequencing libraries are prepared using the TruSeq Stranded Total RNA Library Prep Kit (Illumina, Inc; San Diego, CA). Briefly, ribosomal RNA (rRNA) was depleted from total RNA and the remaining RNA purified, fragmented appropriately, and primed for cDNA synthesis. Blunt-ended cDNA was generated after first and second strand synthesis. Adenylation of the 3' blunt-ends was followed by adapter ligation prior to the enrichment of the cDNA fragments. Final library quality control was carried out by evaluating the fragment size on a DNA1000 chip ran on a 2100 BioAnalyzer (Agilent; Santa Clara, CA). The concentration of each library was determined by quantitative PCR (qPCR) by the KAPA Library Quantification Kit for Next Generation Sequencing (KAPA Biosystems; Woburn, MA) prior to sequencing.

Libraries were normalized to 2 nmol/L in 10 mM Tris-Cl, pH8.5 with 0.1% Tween 20 then pooled evenly. The pooled libraries were denatured with 0.1N NaOH and diluted to 20 pmol/L. Cluster generation of the denatured libraries was performed according to the manufacturer's specifications (Illumina, Inc; San Diego, CA) utilizing the appropriate HiSeq paired-end cluster chemistry and flow cells. Libraries were clustered appropriately with a 1% PhiX spike-in. Sequencing-by-synthesis (SBS) was performed on a HiSeq2500 utilizing the appropriate chemistry with paired-end 101 bp reads. Sequence read data were processed and converted to FASTQ format for downstream analysis by Illumina BaseSpace analysis software, FASTQ Generation v1.0.0.

FASTQ files were processed using the VIPER workflow.(25) Read alignment to human genome build hg19 was performed with STAR.(26) Cufflinks was used to assemble transcript-level expression data from filtered alignments.(27) Differential gene expression analysis was performed using DESeq2.(20) For downstream analyses (GSEA), the RNA-seq matrix was further TMM-normalized using the edgeR package.

RNA-seq/ChIP-seq correlation analysis

To check for concordance between RNA-seq and AR ChIP-seq data, GSEA was used to run the following two analyses:(24)

First, the top 500 most genes with the highest DESeq2 log-fold change in AA versus EA prostate tumors were used as a custom reference gene set. The normalized AR ChIP-seq matrix of AA and EA prostate tumors was used as “expression dataset” input after assigning every peak to the gene with the closest transcriptional start site. Enrichment of AA DE genes in regions of AA-specific AR ChIP-seq signal was tested. Permutation analysis (1000 permutations) was used to generate FDR-corrected p-values.

Second, the top 500 most differentially marked genomic regions based on DESeq2 log-fold change (AA versus EA prostate tumors) were used as a custom gene set, after being assigned to the gene with the closest transcriptional start site. The TMM-normalized RNA-seq matrix of AA and EA prostate tumors was used as “expression dataset” input. Enrichment of AA differentially marked AR ChIP-seq sites around AA DE genes was tested. Permutation analysis (1000 permutations) was used to generate FDR-corrected p-values.

Ancestry score calculation

Genetic ancestry was inferred using common polymorphisms called from off-target and on-target sequencing reads. Germline variant imputation was performed using the STITCH imputation software applied to AR ChIP-seq BAM files for the IP product (merged with the corresponding input control BAMs when available) across all tumor samples.(28) This method leverages ultra-low coverage read data together with the 1000 Genomes reference panel to infer probabilistic germline calls for the autosomal chromosomes. Analysis was restricted to variants with imputation INFO > 0.4 and variant allele frequency (VAF) > 0.01). Ancestry components were inferred for each individual by linear projection using publicly available weights computed by the SNPWEIGHTS software,(29) which had been trained on European, African American, and East Asian individuals in the 1000 Genomes project.(30) The projection was performed using the imputed dosages and the PLINK2 ‘--score’ function to compute the African ancestry component in each sample.

Tissue microarrays

TMAs were previously described.(31) Briefly, TMA were constructed from radical prostatectomy tissues from AA and EA patients operated on at the Michael E. DeBakey VA Medical Center between 1995 and 2013. Patients provided written informed consent for the use of tissues under an Institutional Review Board approved the protocol. Areas of cancer and benign tissue were identified by pathological examination and 1 mm cores of cancer and matched benign tissues from each prostatectomy were used to construct TMAs.

Immunohistochemistry

Immunohistochemistry for FAS was carried out on a Leica BOND III autostainer using online heat treatment with ER1 antigen retrieval solution (citrate pH 6.0) for 20 minutes. Primary antibody incubation was carried out using anti-FAS rabbit monoclonal antibody (Cell Signaling C20G5) at 1:50 dilution for 30 minutes. Detection was carried out using a

Bond Polymer Refine Detection Kit (Leica) for 16 minutes followed by chromogen for 5 minutes. Counterstain was hematoxylin.

Metabolomic profiling

The study cohort has been described previously.(32) Briefly, samples from the Dana-Farber Cancer Institute/Harvard Cancer Center SPORE Prostate Cancer Cohort were used. Fresh-frozen radical prostatectomy specimens from 124 patients were used, with matched normal prostate tissue for 105 out of the 124. Specimens were received fresh from the operating room, inked, sliced, formalin-fixed paraffin embedded (FFPE) and embedded in optimal cutting temperature (OCT) compound and stored in liquid nitrogen. A total of 5-μm-thick sections cut from FFPE and OCT blocks were stained with hematoxylin and eosin (H&E) and examined histologically. Gleason score was assigned based on a representative tumor focus in the corresponding tissue block.

For each individual in the study, approximately 1 mg of tissue was sent to Metabolon, Inc. Metabolon prepared the frozen tissue cores and serum samples for analysis using their proprietary solvent extraction method and internal standards were added to each sample for normalization and quality control. Additional details are described previously.(33)

Metabolites with more than 50% missing values were excluded from the analysis. Data were further corrected for batch effects using median-scaling, normalized using the probabilistic quotient approach,(34) and log2-transformed. Missing values were imputed using a knn-based approach.(35) The preprocessed data included 273 metabolites measured in 124 samples (110 EA and 14 AA). For the differential analysis, only tumor samples from EA and AA patients were used. Differential metabolite abundances were estimated using a linear model (met ~ Race), and the corresponding p-values were corrected for multiple testing using the Benjamini-Hochberg method (FDR<0.2).

Clinical cohort

We used publicly available data on patients with metastatic prostate adenocarcinoma treated with androgen receptor signaling inhibitors (ARSIs).(36) We restricted the analysis to patients who had both clinical and transcriptomic data available (81 patients). We applied ssGSEA to normalized RNA-seq data and extracted sample-level enrichment scores for the Hallmark Fatty Acid Metabolism gene set. The cohort was then split into two groups: top quartile, and lower three quartiles based on ssGSEA enrichment scores. Overall survival (OS) and time to treatment failure (TTF) were compared between the two groups. For OS, patients who were alive were censored at the date of last follow-up. For TTF, patients who were alive without progression and were still on treatment with the same ARSI were censored at the date of last follow-up. The distributions of OS and TTF were estimated with the Kaplan-Meier method along with the corresponding hazard ratios between the two groups, as well 95% confidence intervals. All tests were two-tailed; statistical significance was defined as $P<0.05$. Survival analyses were performed using the “survival” and “survminer” R packages.

Cell culture

LNCaP cells were cultured in RPMI (Gibco #11875–093) medium supplemented with 10% FBS (Gibco #10483) and 1% Pen-Strep. PCa2b Cells were cultured with BRFF-HPC1 media (Athenaes Cat# 0403) supplemented with 20% FBS (Gibco #*10483)* and 1% Pen-Strep. Cell lines were authenticated by STR fingerprinting and routine PCR based mycoplasma testing was carried out using Mycoplasma detection Kit, Alfa Aesar (VWR Cat No. 10067–040).

Quantitative RT-PCR

For q-PCR experiment, 350K LNCaP cells /well were seeded in a 12 well plate with RPMI 1640 phenol-red free media supplemented with 10% Charcoal Stripped FBS and 1% Pen-Strep. For PCa2b cells, 350K cells were seeded in a 12 well plates in BRFF-HPC1 media with 20% FBS and 1 x Pen-Strep with FNC coating. After 48 hours of seeding, cells were transferred to DMEM (Gibco # 11965–092) + 0.1% FBS + 1XPen-Strep and treated after 24 hour of culturing cells in DMEM+0.1%FBS+1XPen-Strep. After 24 hours of seeding, cells were treated with 10nM of R1881 or EtOH (as vehicle control) and after 48 hours of seeding, a subset were treated with 20μM of enzalutamide. Cells were harvested 48 hours later and processed for RNA isolation using RNeasy Micro Kit (Qiagen#74004). cDNA was made from 500ng of total RNA using High-Capacity cDNA Reverse Transcription Kit (Thermo Fisher Scientific#4368814). Gene expression of specific target genes were analyzed using the primers mentioned below and Power SYBR Green PCR master mix (Applied Biosystems#4367659) with Quantstudio3 Real-Time PCR System (Applied Biosystems). qPCR data were analyzed by the $2^{-\Delta\Delta Ct}$ method using 18S rRNA as the reference transcript and gene expression of the treatment groups were represented as the fold change in comparison to the vehicle treated cells. Primer sequences were as follows: *18S* (forward: ACCGCAGCTAGGAATAATGGA; reverse: GCCTCAGTTCCGAAAACCA), *KLK3* (forward: ACCTGCACCCGGAGAGCT; reverse: TCACGGACAGGGTGAGGAAG), *FASN* (forward: TTCTACGGCTCCACGCTCTTCC; reverse: GAAGAGTCTTCGTCAGCCAGGA). To examine expression of mRNA we carried out quantitative real-time RT-PCR (Q-RT-PCR on an Applied Biosystems StepOne (Life Technologies). Following total RNA extraction, cDNA was synthesized using an iScript cDNA Synthesis kit (BioRad) with OligodT in a PTC-200 thermocycler (5 min at 25°C; 30 min at 42°C; 5 min at 85°C). FASN, and β-actin TaqMan probes (ABI) were utilized. PCR conditions were set using standard 2-step manufacturer's protocol. Differences in mRNA levels were analyzed using the 2−ΔΔCT method normalized to β-actin expression. Each measurement point was repeated at least in duplicate.

Data Availability

The ChIP-seq data for patient samples has been deposited in GEO (GSE181440 and GSE181441). The RNA-seq, and metabolomic data for patient samples that support the findings of this study are available upon request from the corresponding authors (M.L.F. and S.K.) to comply with institutional ethics regulations to protect patient privacy. All requests for raw and analyzed data will be promptly reviewed to verify if the request is subject to any

intellectual property or confidentiality obligations. Any data and materials that can be shared will be released via a Data Transfer Agreement.

RESULTS

The AR cistrome is reprogrammed in prostate tumorigenesis in AA men

We generated and analyzed AR ChIP-seq data on 23 human prostate tissue specimens including 9 PCa and histologically normal prostate samples from AA men and 5 PCa samples from EA men (Methods; Supplementary Table 1). Self-reported ancestry was confirmed through genotyping (Supplementary Fig. 1). The AA prostate AR cistrome undergoes extensive reprogramming during tumorigenesis, similar to what we previously observed in EA men (Fig. 1a).(11) As expected, AR binding sites (ARBS) with greater intensity across AA tumors relative to normal specimens were highly enriched for genes upregulated in PCa (Fig. 1b-c).

Differences in the PCa AR cistrome between AA and EA men associate with distinct RNA expression programs

To interrogate whether tumor AR binding patterns differ by ancestry, we performed an unsupervised analysis of the PCa AR cistromes, which clustered clearly into AA and EA groups (Fig. 2a). 118,467 and 115,584 ARBS were identified in AA and EA PCa, respectively. Although the total number of ARBS was similar, 16,678 demonstrated significantly greater binding intensity in AA relative to EA PCa (AA-ARBS), while only 1,655 demonstrated greater binding intensity in EA PCa (EA-ARBS) (Fig. 2b; Methods).

We next sought to evaluate whether ancestry-enriched AR binding associates with differential RNA expression. We performed RNA-seq on an independent set of paired tumor-normal prostate specimens from 30 AA men and 19 EA men, identifying 466 genes upregulated and 729 downregulated in AA relative to EA PCa (Fig. 2c; Supplementary Tables 2-4). We observed a strong overall correlation between epigenomic and transcriptomic data. Using gene set enrichment analysis (GSEA), transcripts nearest AA-ARBS were enriched for genes upregulated in AA relative to EA PCa in the RNA-seq data (normalized enrichment score [NES] = 1.96; $P < 0.001$) (Fig. 2d). Likewise, genes with higher expression in AA than EA tumors were enriched for AA-ARBS (NES = 2.04; $P < 0.001$) (Fig. 2e), suggesting that a significant portion of differential gene expression between AA and EA PCa may be driven by ancestral differences in AR binding.

The AR PCa cistrome associates with lipid metabolism and immune response

To investigate biological processes associated with ancestral differences in the PCa AR cistromes, we first performed motif analysis on the EA-ARBS and AA-ARBS (Fig. 3a). Motifs for the transcription factors (TFs) HOXD13, FOXA1, and PGR (progesterone receptor) were enriched in EA-ARBS. HOXB13, which shares a nearly identical motif with HOXD13, and FOXA1 are known to co-localize to ARBS in PCa in EA men.(11) Motifs for Sp1, Elk4, and NRF1 were enriched in AA-ARBS. Sp1 is a TF reported to co-localize with AR and regulate *de novo* lipogenesis and proliferation in PCa cells.(37,38) NRF1 is a TF reported to be a co-activator of AR and regulates key metabolic genes to cellular growth.(39)

Elk4 is an ETS family TF that is highly expressed in a subset of prostate cancer and is involved in promoting cell growth.(40)

We next analyzed the AA-ARBS using CISTROME-GO, a tool that performs functional enrichment analysis of TF ChIP-seq peaks.(23) Three of the top ten most enriched gene sets, including the top overall gene set, pertained to lipid metabolism (Fig. 3b). Using single-sample GSEA (ssGSEA), we observed greater and more consistent AR binding intensity at KEGG lipid metabolism gene sets across AA compared to EA PCa samples (Fig. 3c). Consistent with the strong global correlation between ancestry-enriched AR binding sites and RNA expression, we observed that greater AR binding intensity at lipid metabolism genes was associated with transcriptional upregulation of these pathways in our independent RNA-seq dataset (Fig. 3d; Supplementary Tables 3-4). Notably, immune response and cytokine signaling were also strongly represented in the list of pathways enriched in AA-ARBS, comprising 12 of the 20 top gene sets (Fig. 3b). ssGSEA demonstrated greater and more consistent AR binding intensity at KEGG immune gene sets across AA compared to EA PCa samples (Fig. 3e). In our independent RNA-seq dataset, several immune response gene sets were significantly upregulated in AA versus EA PCa (Fig. 3f). Further, applying TIMER2.0, which provides quantitative estimates of six tumor-infiltrating immune subsets, to our RNA-seq demonstrated a significantly higher signal for B-cells ($P = 0.01$) and macrophages ($P = 0.003$), and a trend towards CD8+ T-cells ($P = 0.051$) (Fig. 3g).(41) These findings are concordant with previously published differential gene expression analyses comparing AA and EA prostate tumors, most of which identified upregulation of lipid metabolism, immune response, and/or cytokine signaling gene sets in AA versus EA PCa.(4,42–48) Our data implicate differential AR binding as a potential driver of these distinct transcriptional programs. Results of CISTROME-GO analysis of the EA-ARBS are shown in Supplementary Table 5.

Multiomic analysis demonstrates upregulated lipid metabolism in AA PCa

We next assessed differential AR binding at individual genes. Each gene was assigned a regulatory potential (RP) score – a quantitative value reflecting the likelihood that a set of TF ChIP-seq peaks are a direct regulator of a given gene.(23) The gene with the second highest RP score in the AA-ARBS was *FASN*, which encodes fatty acid synthase (FAS), a critical catalytic enzyme in fatty acid synthesis whose expression is associated with aggressive PCa (Fig. 4a; Supplementary Table 6).(49–51) The gene with the highest RP score was *SNORD134*, an uncharacterized small nucleolar RNA embedded in intron 11 of the *FASN* gene. Visualization of AR binding at the *FASN* locus in the 14 prostate tumors clearly demonstrates greater binding intensity at the *FASN* promoter in prostate tumors from AA men (Fig 4b). Notably, several additional genes encoding key lipid metabolism proteins, including *SREBF1* (sterol regulatory element binding transcription factor 1), *SCD* (stearoyl-CoA desaturase), *SLC25A1* (citrate transport protein), ACLY (ATP citrate lyase), and *ACACA* (acetyl-CoA carboxylase alpha) exhibited greater AR binding intensity at their gene promoters in AA versus EA PCa (Fig. 4b).

Consistent with published transcriptomic data and greater AR binding intensity at the *FASN* promoter in AA PCa, an independent cohort of 48 samples demonstrated higher

FASN expression in AA (n=24) than EA tumors (n=24) (P = 0.022) (Fig. 4c).(4) *FASN* expression was higher in PCa compared to normal prostate tissue in both ancestral groups. To evaluate the regulatory relationship between AR and *FASN* expression, we treated two cell lines – LNCaP and PCA2b, the only AA-derived PCa cell line – with or without the synthetic androgen R1881. As expected, we observed R1881-mediated upregulation of *KLK3*, a canonical AR-regulated gene, in both cell lines (Fig. 4d). In response to androgen stimulation, *FASN* mRNA levels also increased in both cell lines. Subsequent treatment with the AR antagonist enzalutamide abrogated androgen-induced upregulation of both genes (Fig. 4d), confirming that AR regulates *FASN* gene expression *in vitro*.

Whether enhanced *FASN* expression translates into higher FAS protein expression in AA PCa is not known. To characterize FAS protein levels, we performed immunohistochemistry on an independent set of 492 prostate tissue samples, including 102 tumor and 112 normal specimens from AA men and 150 tumor and 128 normal specimens from EA men. We observed significantly greater FAS protein levels in tumors compared to normal specimens for both ancestral groups (Fig. 4e). Comparison of AA versus EA tumors demonstrated significantly higher FAS protein levels in AA PCa (P = 0.0011). Notably, there was no difference in *FASN* RNA or FAS protein levels in normal prostate tissue from AA and EA men.

Based on results of this integrated analysis, we speculated that upregulation of FAS would translate to higher lipid levels in AA PCa. We therefore performed metabolic profiling in an independent cohort of 14 AA and 110 EA prostate tumors. Sixty-five (69%) of 94 lipids, including 26 (79%) of 33 fatty acids, demonstrated numerically higher levels in AA than EA PCa; 9 lipids, including 4 fatty acids, were present at significantly higher levels (Fig. 4f). These data add to a growing literature demonstrating an altered lipid metabolic profile in AA PCa.(52,53) This may be biologically and clinically relevant as PCa cells upregulate *de novo* lipogenesis to support rapid cellular division, increased uptake of exogenous lipids is linked to PCa aggressiveness, and high-fat diets and obesity are associated with PCa incidence and progression.(54)

Upregulated lipid metabolism is associated with aggressive PCa

While previous studies have demonstrated an association between altered lipid metabolism and PCa aggressiveness in pre-clinical models, its relation to clinical outcomes in men with PCa is not well defined.(55,56) To investigate the clinical implications of upregulated lipogenesis, we analyzed publicly available transcriptomic and clinical data from men with metastatic PCa. We applied ssGSEA to normalized RNA-seq data and extracted sample-level enrichment scores for the Hallmark Fatty Acid Metabolism gene set in 81 men with metastatic PCa.(36) Greater expression of the 160 genes in the Hallmark Fatty Acid Metabolism gene set was associated with significantly shorter progression-free survival to first-line AR signaling inhibitors (ARSIs), abiraterone or enzalutamide, (hazard ratio [HR] = 1.8, 95% confidence interval [CI]: 1.0–3.2; P = 0.04) and overall survival (HR = 2.8, 95% CI: 1.5–5.2; P = 0.0005) (Fig. 5a-b). This is the first demonstration in a contemporary metastatic PCa cohort that high expression of lipid metabolism genes is associated with poor response to ARSIs and shorter survival.

DISCUSSION

This study presents the first description of the AR cistrome in primary PCa from AA men, resulting in important biological and clinical observations. There are three key findings of the present research. First, we demonstrate clear differences in the PCa AR cistrome between AA and EA men. Second, our data suggest that these epigenetic differences may contribute to distinct RNA expression programs in AA and EA PCa. The third key finding is that sites with greater AR binding intensity in AA PCa are enriched for lipid metabolism genes with concomitant upregulation of lipogenic activity. Given the substantial association of upregulated lipid metabolism with PCa aggressiveness, this provides a plausible role for differential AR binding in contributing to PCa disparities.

Epigenetics provides a potential link between ancestry, environment, and cancer biology. The finding that approximately 75% of variation in DNA methylation is explained by genomic ancestry suggests that environmental factors not captured by ancestry also contribute to epigenomic variation.(57) Indeed, compelling data supports that factors experienced differently across ancestral groups, such as diet, can modify the epigenome.(58) The evolving understanding of epigenetics at the intersection of ancestry, environment, and biology highlights the importance of understanding epigenetic differences across ancestral groups for mitigating PCa racial disparities.

The role of the AR in PCa initiation and progression is well-established, yet how the PCa AR cistrome differs across men of different ancestry is not known. We previously demonstrated that the AR cistrome is extensively reprogrammed in PCa tumorigenesis and disease progression.(11,12) Further, differences in the AR cistrome across states generated novel mechanistic insights into events driving normal prostate cells to undergo malignant transformation. Reflective of a broader issue of underrepresentation of samples from minority populations in molecular cancer research, this data was generated exclusively in EA men. Herein, we report that the PCa AR cistrome is also extensively reprogrammed in AA men. This finding has two important implications. First, it solidifies epigenetic reprogramming as central to human prostate tumorigenesis, irrespective of ancestry. Second, it provides a novel opportunity to identify differences in PCa biology between AA and EA men. Comparative analyses across several molecular features have identified ancestry-specific genetic risk and somatic variants, and differences in RNA expression, tumor microenvironment, and androgen levels between AA and EA men.(3–7) This paper provides the first insights into how differences in AR binding may contribute to observed racial disparities and identify novel therapeutic strategies to improve PCa outcomes for AA men.

We observed that differences in AR binding between AA and EA men is associated with distinct RNA expression programs. Consistent with its known role as a direct regulator of gene transcription, we observed global upregulation of genes in AA PCa near AA-ARBS as well as greater AR binding intensity near genes upregulated in AA PCa. These results imply that a significant portion of differential gene expression between AA and EA PCa may be driven by ancestral differences in AR binding. This novel finding provides the first suggestion that divergence in the AR cistrome, and likely other epigenetic features, may underlie differences in PCa biology between AA and EA men. This idea is further

supported by the observation that the top two biological processes enriched in AA-ARBS, lipid metabolism and immune response/cytokine signaling, are upregulated in AA versus EA PCa in prior comparative transcriptomic analyses.(4,42–48) Notably, a recent study reported greater expression of genes involved in adipogenesis in EA than AA PCa.(43) However, the effect size was modest and this report comprised a single dataset. In comparison, we observed evidence of upregulated lipid metabolism in AA PCa across independent epigenomic, transcriptomic, and metabolomic datasets.

Higher expression of lipid metabolism genes in our RNA-seq dataset and lipids and fatty acids in our metabolomic dataset in PCa from AA versus EA men adds to the literature supporting an altered lipid metabolic profile in PCa in AA men.(4,52,53) Further, we report three novel findings that add to our understanding of differences in the lipid metabolism pathway in AA PCa and its potential clinical implications. The first is that AA PCa exhibits greater AR binding intensity at lipid metabolism genes. The role of AR in upregulating aberrant lipogenesis is supported by our *in vitro* experiments demonstrating a regulatory relationship between AR signaling and *FASN* expression in an AA PCA cell line. The second discovery pertains to *FASN*, which encodes fatty acid synthase (FAS), a critical catalytic enzyme in lipid metabolism that is associated with aggressive PCa.(49–51) *FASN* has been previously shown to be upregulated in PCa in AA versus EA men, but whether this correlates with increased FAS protein expression was not known.(4) We show for the first time that FAS protein levels are significantly elevated in PCa in AA versus EA men. It's notable that while *FASN* RNA and FAS protein levels were significantly higher in AA than EA PCa, there was no difference in either in normal prostate tissue between ancestral groups. The absence of difference in normal prostate tissue suggests that FAS upregulation in AA PCa is likely independent of external factors, such as differences in diet, that may be experienced differently by AA and EA men.

The third observation in this study pertains to the clinical implications of upregulated lipid metabolism. While pre-clinical models demonstrate its association with aggressive PCa, upregulated lipid metabolism is not known to impact clinical outcomes in men with PCa.(55,56) Our data suggest that higher expression of lipid metabolism genes is associated with poor response to ARSIs and shorter survival in a contemporary metastatic PCa cohort. This finding further strengthens the rationale for inhibiting lipid metabolism as a novel therapeutic approach in men with PCa and suggests that AA men may be more likely to benefit from these drugs. We previously demonstrated that the selective FAS inhibitor IPI-9119 reduces tumor growth in CRPC preclinical models and human organoids.(49) With drugs targeting FAS and other lipid metabolism enzymes in clinical development, we urge clinical trials to enroll diverse patient populations. Additionally, correlative studies to identify biomarkers, such as FAS protein levels and/or lipid metabolism gene expression, will be critical to identify patients most likely to benefit from this treatment approach.

In addition to lipid metabolism, AR binding sites with greater intensity in PCa in AA men demonstrated a strong enrichment for immune response and cytokine signaling genes. While epigenetic regulation of immune response is well-established, our data is the first to suggest that differences in the PCa tumor microenvironment between AA and EA men may be driven in part by differential AR binding.(59) This novel finding was concordant

with greater expression of immune response and cytokine signaling gene sets in our independent RNA-seq dataset, which is consistent with results of several comparative transcriptomic analyses.(4,42–48) Provocative data suggests a potential clinical correlation of this differential immune response between AA and EA men with PCa. Sipuleucel-T is an autologous cellular immunotherapy demonstrated to prolong survival in men with metastatic PCa.(60) Analysis of the PROCEED Registry demonstrated that AA men treated with Sipuleucel-T lived significantly longer than EA men.(61) Our RNA-seq data also demonstrated greater intra-tumoral activity of macrophages, B-cells, and CD8+ T-cells, all of which are involved in the immune response to Sipuleucel-T.(62) The prostate tumor microenvironment may have clinical implications beyond response to immunotherapy. A recent report suggests that tumor-associated macrophages promote castration-resistance by contributing cholesterol for intra-tumoral androgen production.(63) In light of our findings, further studies are warranted to explore the relationship between tumor microenvironment, lipid metabolism, and androgen signaling in PCa across men of different ancestry.

While the present results strongly support the conclusions discussed herein, it is appropriate to recognize potential limitations. First, the small sample size of the AR ChIP-seq cohort is modest. Additionally, due to limitations in tissue availability, we were unable to perform DNA-seq or RNA-seq on the same samples that underwent AR ChIP-seq analysis. This precluded our ability to correlate the AR ChIP-seq results with other molecular features that can alter AR signaling, such as *ERG* fusion status and CAG repeats, which are known to differ between AA and EA men. However, the results of the differential AR binding analysis identified biological processes corroborated by our independent RNA-seq and metabolomic cohorts, as well as published data, strongly supports the epigenetic findings. Another limitation is that AR was the only epigenetic feature evaluated in this study. Other TFs, such as FOXA1 and HOXB13, and histone modifications clearly play a role in PCa development.(13,14) It will be important that future studies integrate comprehensive epigenetic profiling with RNA-seq and DNA-seq data. Performing these analyses within the same samples will provide clarity on how genomic alterations influence epigenetics, the regulatory relationship between epigenetic features and RNA expression, and how these differences contribute to prostate cancer racial disparities.

In summary, our data suggest a model whereby differential androgen signaling may contribute to higher levels of lipid metabolism, immune response, and cytokine signaling in AA prostate tumors. Given the substantial association of upregulated lipogenesis with PCa progression, our study provides a plausible biological explanation of the higher incidence and aggressiveness of PCa observed in AA men.(1,2,64,65) With inhibitors of key lipid metabolism enzymes as well as immunotherapies in clinical development, our findings suggest a potential therapeutic opportunity to target and attenuate racial disparities in PCa. Further exploration of these treatment approaches in pre-clinical AA PCa models and enrollment of diverse patient populations in future clinical trials is warranted. In conclusion, this study offers the first insights into ancestry-specific differences in the PCa AR cistrome. More broadly, our study demonstrates the utility of epigenomic approaches to gain insight into the biological differences underlying cancer disparities.

Supplementary Material

Refer to Web version on PubMed Central for supplementary material.

ACKNOWLEDGMENTS

J.E.B. is supported by the Department of Defense (W81XWH-20-1-0118). S.C.B. is supported by a Young Investigator Award from the American Society of Clinical Oncology and a fellowship from the PhRMA Foundation and the Kure It Cancer Research Foundation. D.L. and C.M. are supported by the National Institute of General Medical Sciences of the National Institutes of Health under Award Number T32GM136554 and T32GM008231. M.L. is supported by the NIH (RO1CA131945), Department of Defense (PC160357, PC180582, P50CA211024), and the Prostate Cancer Foundation. M.L.F. is supported by the Claudia Adams Barr Program for Innovative Cancer Research, the H.L. Snyder Medical Research Foundation, and the Cutler Family Fund for Prevention and Early Detection. N.M., M.I., and S.K. are supported by the Prostate Cancer Foundation Young Investigator and Challenge Awards, the National Cancer Institute U54-CA233223, and the Department of Defense PCRP IDA W81XWH-18-1-0288 and PCRP HDRA W81XWH2110253.

REFERENCES

1. Farkas A, Marcella S, Rhoads GG. Ethnic and racial differences in prostate cancer incidence and mortality. Ethn Dis. 2000;10:69–75. [PubMed: 10764132]
2. Fowler JE, Bigler SA, Bowman G, Kilambi NK. Race and cause specific survival with prostate cancer: influence of clinical stage, Gleason score, age and treatment. J Urol. 2000;163:137–42. [PubMed: 10604331]
3. Mahal BA, Alshalalfa M, Kensler KH, Chowdhury-Paulino I, Kantoff P, Mucci LA, et al. Racial Differences in Genomic Profiling of Prostate Cancer. New England Journal of Medicine. Massachusetts Medical Society; 2020;383:1083–5.
4. Powell IJ, Dyson G, Land S, Ruterbusch J, Bock CH, Lenk S, et al. Genes associated with prostate cancer are differentially expressed in African American and European American men. Cancer Epidemiol Biomarkers Prev. 2013;22:891–7. [PubMed: 23515145]
5. Gaston KE, Kim D, Singh S, Ford OH, Mohler JL. Racial differences in androgen receptor protein expression in men with clinically localized prostate cancer. J Urol. 2003;170:990–3. [PubMed: 12913756]
6. Freedman ML, Haiman CA, Patterson N, McDonald GJ, Tandon A, Waliszewska A, et al. Admixture mapping identifies 8q24 as a prostate cancer risk locus in African-American men. Proc Natl Acad Sci U S A. 2006;103:14068–73. [PubMed: 16945910]
7. Conti DV, Darst BF, Moss LC, Saunders EJ, Sheng X, Chou A, et al. Trans-ancestry genome-wide association meta-analysis of prostate cancer identifies new susceptibility loci and informs genetic risk prediction. Nat Genet. 2021;53:65–75. [PubMed: 33398198]
8. Kwabi-Addo B, Wang S, Chung W, Jelinek J, Patierno SR, Wang B-D, et al. Identification of differentially methylated genes in normal prostate tissues from African American and Caucasian men. Clin Cancer Res. 2010;16:3539–47. [PubMed: 20606036]
9. Devaney JM, Wang S, Furbert-Harris P, Apprey V, Ittmann M, Wang B-D, et al. Genome-wide differentially methylated genes in prostate cancer tissues from African-American and Caucasian men. Epigenetics. 2015;10:319–28. [PubMed: 25864488]
10. Rubicz R, Zhao S, Geybels M, Wright JL, Kolb S, Klotzle B, et al. DNA methylation profiles in African American prostate cancer patients in relation to disease progression. Genomics. 2019;111:10–6. [PubMed: 26902887]
11. Pomerantz MM, Li F, Takeda DY, Lenci R, Chonkar A, Chabot M, et al. The androgen receptor cistrome is extensively reprogrammed in human prostate tumorigenesis. Nat Genet. 2015;47:1346–51. [PubMed: 26457646]
12. Pomerantz MM, Qiu X, Zhu Y, Takeda DY, Pan W, Baca SC, et al. Prostate cancer reactivates developmental epigenomic programs during metastatic progression. Nat Genet. 2020;52:790–9. [PubMed: 32690948]

13. Parolia A, Cieslik M, Chu S-C, Xiao L, Ouchi T, Zhang Y, et al. Distinct structural classes of activating FOXA1 alterations in advanced prostate cancer. Nature. 2019;571:413–8. [PubMed: 31243372]
14. Ewing CM, Ray AM, Lange EM, Zuhlke KA, Robbins CM, Tembe WD, et al. Germline Mutations in HOXB13 and Prostate-Cancer Risk. N Engl J Med. 2012;366:141–9. [PubMed: 22236224]
15. Langmead B, Trapnell C, Pop M, Salzberg SL. Ultrafast and memory-efficient alignment of short DNA sequences to the human genome. Genome Biology. 2009;10:R25. [PubMed: 19261174]
16. Zhang Y, Liu T, Meyer CA, Eeckhoute J, Johnson DS, Bernstein BE, et al. Model-based analysis of ChIP-Seq (MACS). Genome Biol. 2008;9:R137. [PubMed: 18798982]
17. Cavalcante RG, Sartor MA. annotatr: genomic regions in context. Bioinformatics. Oxford Academic; 2017;33:2381–3.
18. Robinson JT, Thorvaldsdóttir H, Winckler W, Guttman M, Lander ES, Getz G, et al. Integrative genomics viewer. Nat Biotechnol. 2011;29:24–6. [PubMed: 21221095]
19. Köster J, Rahmann S. Snakemake--a scalable bioinformatics workflow engine. Bioinformatics. 2012;28:2520–2. [PubMed: 22908215]
20. Love MI, Huber W, Anders S. Moderated estimation of fold change and dispersion for RNA-seq data with DESeq2. Genome Biology. 2014;15:550. [PubMed: 25516281]
21. Heinz S, Benner C, Spann N, Bertolino E, Lin YC, Laslo P, et al. Simple combinations of lineage-determining transcription factors prime cis-regulatory elements required for macrophage and B cell identities. Mol Cell. 2010;38:576–89. [PubMed: 20513432]
22. McLean CY, Bristor D, Hiller M, Clarke SL, Schaar BT, Lowe CB, et al. GREAT improves functional interpretation of cis-regulatory regions. Nat Biotechnol. 2010;28:495–501. [PubMed: 20436461]
23. Li S, Wan C, Zheng R, Fan J, Dong X, Meyer CA, et al. Cistrome-GO: a web server for functional enrichment analysis of transcription factor ChIP-seq peaks. Nucleic Acids Res. 2019;47:W206–11. [PubMed: 31053864]
24. Subramanian A, Tamayo P, Mootha VK, Mukherjee S, Ebert BL, Gillette MA, et al. Gene set enrichment analysis: A knowledge-based approach for interpreting genome-wide expression profiles. PNAS. National Academy of Sciences; 2005;102:15545–50.
25. Cornwell M, Vangala M, Taing L, Herbert Z, Köster J, Li B, et al. VIPER: Visualization Pipeline for RNA-seq, a Snakemake workflow for efficient and complete RNA-seq analysis. BMC Bioinformatics. 2018;19:135. [PubMed: 29649993]
26. Dobin A, Davis CA, Schlesinger F, Drenkow J, Zaleski C, Jha S, et al. STAR: ultrafast universal RNA-seq aligner. Bioinformatics. 2013;29:15–21. [PubMed: 23104886]
27. Trapnell C, Roberts A, Goff L, Pertea G, Kim D, Kelley DR, et al. Differential gene and transcript expression analysis of RNA-seq experiments with TopHat and Cufflinks. Nat Protoc. 2012;7:562–78. [PubMed: 22383036]
28. Davies RW, Flint J, Myers S, Mott R. Rapid genotype imputation from sequence without reference panels. Nat Genet. 2016;48:965–9. [PubMed: 27376236]
29. Chen C-Y, Pollack S, Hunter DJ, Hirschhorn JN, Kraft P, Price AL. Improved ancestry inference using weights from external reference panels. Bioinformatics. 2013;29:1399–406. [PubMed: 23539302]
30. Auton A, Abecasis GR, Altshuler DM, Durbin RM, Abecasis GR, Bentley DR, et al. A global reference for human genetic variation. Nature. 2015;526:68–74. [PubMed: 26432245]
31. Wong M, Bierman Y, Pettaway C, Kittles R, Mims M, Jones J, et al. Comparative analysis of p16 expression among African American and European American prostate cancer patients. Prostate. 2019;79:1274–83. [PubMed: 31111520]
32. Penney KL, Tyekucheva S, Rosenthal J, El Fandy H, Carelli R, Borgstein S, et al. Metabolomics of Prostate Cancer Gleason Score in Tumor Tissue and Serum. Mol Cancer Res. 2021;19:475–84. [PubMed: 33168599]
33. Cacciatore S, Zadra G, Bango C, Penney KL, Tyekucheva S, Yanes O, et al. Metabolic Profiling in Formalin-Fixed and Paraffin-Embedded Prostate Cancer Tissues. Mol Cancer Res. 2017;15:439–47. [PubMed: 28074002]

34. Dieterle F, Ross A, Schlotterbeck G, Senn H. Probabilistic quotient normalization as robust method to account for dilution of complex biological mixtures. Application in 1H NMR metabonomics. Anal Chem. 2006;78:4281–90. [PubMed: 16808434]
35. Do KT, Wahl S, Raffler J, Molnos S, Laimighofer M, Adamski J, et al. Characterization of missing values in untargeted MS-based metabolomics data and evaluation of missing data handling strategies. Metabolomics. 2018;14:128. [PubMed: 30830398]
36. Abida W, Cyrta J, Heller G, Prandi D, Armenia J, Coleman I, et al. Genomic correlates of clinical outcome in advanced prostate cancer. Proc Natl Acad Sci USA. 2019;116:11428–36. [PubMed: 31061129]
37. Tewari AK, Yardimci GG, Shibata Y, Sheffield NC, Song L, Taylor BS, et al. Chromatin accessibility reveals insights into androgen receptor activation and transcriptional specificity. Genome Biology. 2012;13:R88. [PubMed: 23034120]
38. Lu S, Archer MC. Sp1 coordinately regulates de novo lipogenesis and proliferation in cancer cells. International Journal of Cancer. 2010;126:416–25. [PubMed: 19621387]
39. Schultz MA, Hagan SS, Datta A, Zhang Y, Freeman ML, Sikka SC, et al. Nrf1 and Nrf2 Transcription Factors Regulate Androgen Receptor Transactivation in Prostate Cancer Cells. PLOS ONE. Public Library of Science; 2014;9:e87204.
40. Rickman DS, Pflueger D, Moss B, VanDoren VE, Chen CX, de la Taille A, et al. SLC45A3-ELK4 is a novel and frequent erythroblast transformation-specific fusion transcript in prostate cancer. Cancer Res. 2009;69:2734–8. [PubMed: 19293179]
41. Li T, Fu J, Zeng Z, Cohen D, Li J, Chen Q, et al. TIMER2.0 for analysis of tumor-infiltrating immune cells. Nucleic Acids Res. 2020;48:W509–14. [PubMed: 32442275]
42. Wallace TA, Prueitt RL, Yi M, Howe TM, Gillespie JW, Yfantis HG, et al. Tumor immunobiological differences in prostate cancer between African-American and European-American men. Cancer Res. 2008;68:927–36. [PubMed: 18245496]
43. Rayford W, Beksac AT, Alger J, Alshalalfa M, Ahmed M, Khan I, et al. Comparative analysis of 1152 African-American and European-American men with prostate cancer identifies distinct genomic and immunological differences. Commun Biol. 2021;4:670. [PubMed: 34083737]
44. Kinseth MA, Jia Z, Rahmatpanah F, Sawyers A, Sutton M, Wang-Rodriguez J, et al. Expression differences between African American and Caucasian prostate cancer tissue reveals that stroma is the site of aggressive changes. Int J Cancer. 2014;134:81–91. [PubMed: 23754304]
45. Hardiman G, Savage SJ, Hazard ES, Wilson RC, Courtney SM, Smith MT, et al. Systems analysis of the prostate transcriptome in African-American men compared with European-American men. Pharmacogenomics. 2016;17:1129–43. [PubMed: 27359067]
46. Rahmatpanah F, Robles GD, Lilly M, Keane T, Kumar V, Mercola D, et al. RNA expression differences in prostate tumors and tumor-adjacent stroma between Black and White Americans. Oncotarget. Impact Journals; 2021;12:1457–69.
47. Awasthi S, Berglund A, Abraham-Miranda J, Rounbehler RJ, Kensler K, Serna A, et al. Comparative Genomics Reveals Distinct Immune-oncologic Pathways in African American Men with Prostate Cancer. Clin Cancer Res. 2021;27:320–9. [PubMed: 33037017]
48. Yuan J, Kensler KH, Hu Z, Zhang Y, Zhang T, Jiang J, et al. Integrative comparison of the genomic and transcriptomic landscape between prostate cancer patients of predominantly African or European genetic ancestry. PLoS Genet. 2020;16:e1008641.
49. Zadra G, Ribeiro CF, Chetta P, Ho Y, Cacciatore S, Gao X, et al. Inhibition of de novo lipogenesis targets androgen receptor signaling in castration-resistant prostate cancer. PNAS. National Academy of Sciences; 2019;116:631–40.
50. Epstein JI, Carmichael M, Partin AW. OA-519 (fatty acid synthase) as an independent predictor of pathologic state in adenocarcinoma of the prostate. Urology. 1995;45:81–6. [PubMed: 7817483]
51. Bastos DC, Ribeiro CF, Ahearn T, Nascimento J, Pakula H, Clohessy J, et al. Genetic ablation of FASN attenuates the invasive potential of prostate cancer driven by Pten loss. J Pathol. 2021;253:292–303. [PubMed: 33166087]
52. Zhou X, Mei H, Agee J, Brown T, Mao J. Racial differences in distribution of fatty acids in prostate cancer and benign prostatic tissues. Lipids Health Dis. 2019;18:189. [PubMed: 31677641]

53. Figiel S, Pinault M, Domingo I, Guimaraes C, Guibon R, Besson P, et al. Fatty acid profile in peri-prostatic adipose tissue and prostate cancer aggressiveness in African-Caribbean and Caucasian patients. Eur J Cancer. 2018;91:107–15. [PubMed: 29413967]
54. Bader DA, McGuire SE. Tumour metabolism and its unique properties in prostate adenocarcinoma. Nat Rev Urol. 2020;17:214–31. [PubMed: 32112053]
55. Lounis MA, Péant B, Leclerc-Desaulniers K, Ganguli D, Daneault C, Ruiz M, et al. Modulation of de Novo Lipogenesis Improves Response to Enzalutamide Treatment in Prostate Cancer. Cancers (Basel). 2020;12:3339. [PubMed: 33187317]
56. Han W, Gao S, Barrett D, Ahmed M, Han D, Macoska JA, et al. Reactivation of androgen receptor-regulated lipid biosynthesis drives the progression of castration-resistant prostate cancer. Oncogene. 2018;37:710–21. [PubMed: 29059155]
57. Galanter JM, Gignoux CR, Oh SS, Torgerson D, Pino-Yanes M, Thakur N, et al. Differential methylation between ethnic sub-groups reflects the effect of genetic ancestry and environmental exposures. eLife [Internet]. [cited 2021 Jun 11];6. Available from: https://www.ncbi.nlm.nih.gov/pmc/articles/PMC5207770/
58. Zhang Y, Kutateladze TG. Diet and the epigenome. Nature Communications. Nature Publishing Group; 2018;9:3375.
59. Zhang Q, Cao X. Epigenetic regulation of the innate immune response to infection. Nat Rev Immunol. 2019;19:417–32. [PubMed: 30918351]
60. Kantoff PW, Higano CS, Shore ND, Berger ER, Small EJ, Penson DF, et al. Sipuleucel-T Immunotherapy for Castration-Resistant Prostate Cancer. New England Journal of Medicine. Massachusetts Medical Society; 2010;363:411–22.
61. Sartor O, Armstrong AJ, Ahaghotu C, McLeod DG, Cooperberg MR, Penson DF, et al. Survival of African-American and Caucasian men after sipuleucel-T immunotherapy: outcomes from the PROCEED registry. Prostate Cancer Prostatic Dis. 2020;23:517–26. [PubMed: 32111923]
62. Madan RA, Antonarakis ES, Drake CG, Fong L, Yu EY, McNeel DG, et al. Putting the Pieces Together: Completing the Mechanism of Action Jigsaw for Sipuleucel-T. JNCI: Journal of the National Cancer Institute. 2020;112:562–73. [PubMed: 32145020]
63. El-Kenawi A, Dominguez-Viqueira W, Liu M, Awasthi S, Abraham-Miranda J, Keske A, et al. Macrophage-Derived Cholesterol Contributes to Therapeutic Resistance in Prostate Cancer. Cancer Res [Internet]. American Association for Cancer Research; 2021 [cited 2021 Oct 19]; Available from: https://cancerres.aacrjournals.org/content/early/2021/10/13/0008-5472.CAN-20-4028
64. De Piano M, Manuelli V, Zadra G, Otte J, Edqvist P-HD, Pontén F, et al. Lipogenic signalling modulates prostate cancer cell adhesion and migration via modification of Rho GTPases. Oncogene. 2020;39:3666–79. [PubMed: 32139877]
65. Yue S, Li J, Lee S-Y, Lee HJ, Shao T, Song B, et al. Cholesteryl ester accumulation induced by PTEN loss and PI3K/AKT activation underlies human prostate cancer aggressiveness. Cell Metab. 2014;19:393–406. [PubMed: 24606897]

Significance:

With immunotherapies and inhibitors of metabolic enzymes in clinical development, the altered lipid metabolism and immune response in African American men provides potential therapeutic opportunities to attenuate racial disparities in prostate cancer.

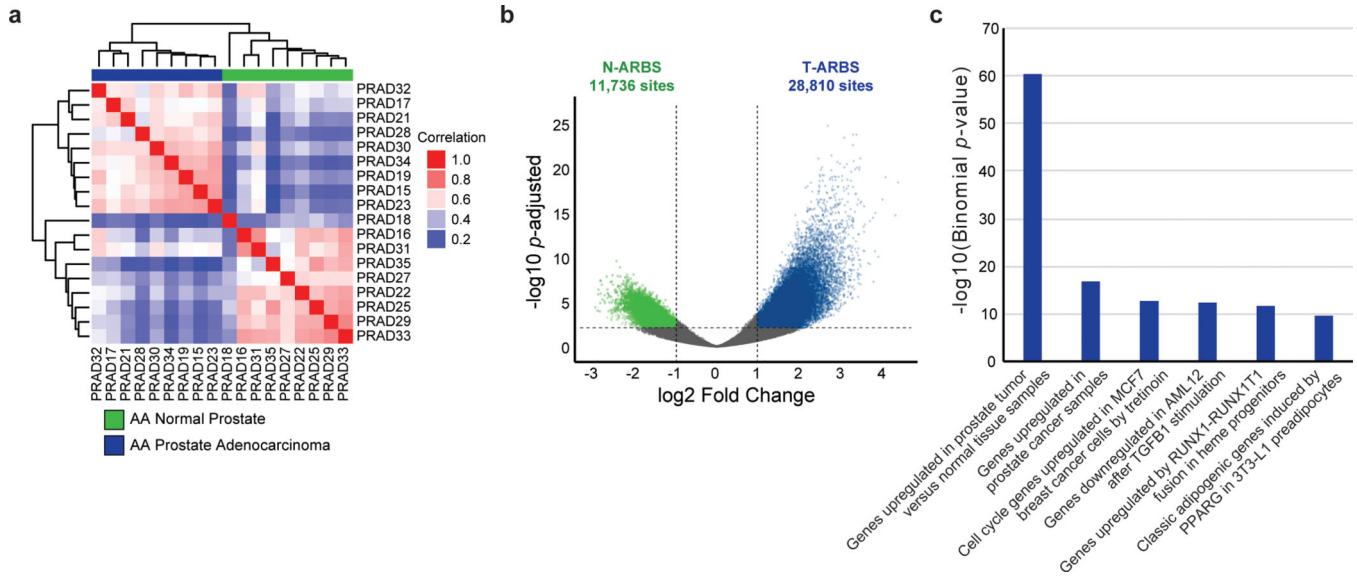

Figure 1.

The AR cistrome is reprogrammed in prostate tumorigenesis in AA men. **a)** Unsupervised pairwise correlation of the AR cistromes from AA prostate tumor and normal specimens. Hierarchical clustering demonstrates the relatedness of each AR cistrome. **b)** Volcano plot of AR binding sites enriched in AA tumor versus normal specimens (T-ARBS; N = 28,810) and normal versus tumor specimens (N-ARBS; N = 11,736) with an FDR-adjusted p-value < 0.01 and log2 fold-change > 1. **c)** MSigDB perturbation pathways enriched in the 28,810 T-ARBS using the GREAT tool.(22)

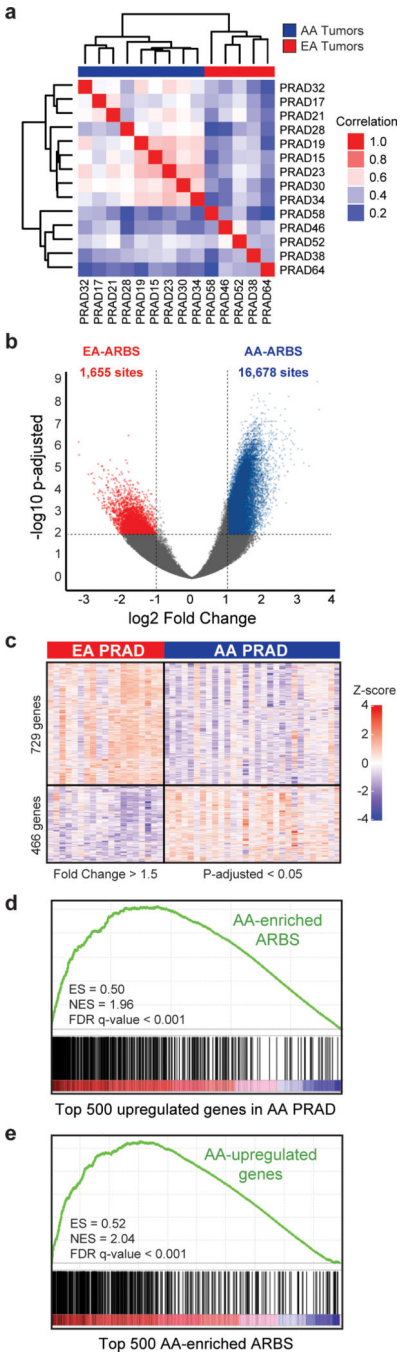

Figure 2.

Differences in the PCa AR cistrome between AA and EA men associate with distinct RNA expression programs. **a)** Unsupervised pairwise correlation of the AR cistromes from AA and EA prostate tumors. Hierarchical clustering demonstrates the relatedness of each AR cistrome. **b)** Volcano plot of ancestry-enriched AR binding sites (ARBS). 16,678 ARBS were enriched in AA relative to EA (AA-ARBS) prostate tumors and 1,655 ARBS in EA relative to AA prostate tumors (EA-ARBS) with an FDR-adjusted p-value < 0.01 and log2 fold-change > 1. **c)** Differential gene expression analysis of 30 AA and 19 EA

paired tumor-normal prostate specimens. 466 genes were upregulated in AA and 729 genes were upregulated in EA prostate tumors with an FDR-adjusted p-value < 0.05 and log2 fold-change > 1.5. **d)** GSEA of AA-ARBS are enriched for genes upregulated in AA relative to EA prostate tumors (normalized enrichment score [NES] = 1.96; P < 0.001). **e)** GSEA of genes upregulated in AA prostate tumors are enriched for AA-ARBS (NES = 2.04; P < 0.001).

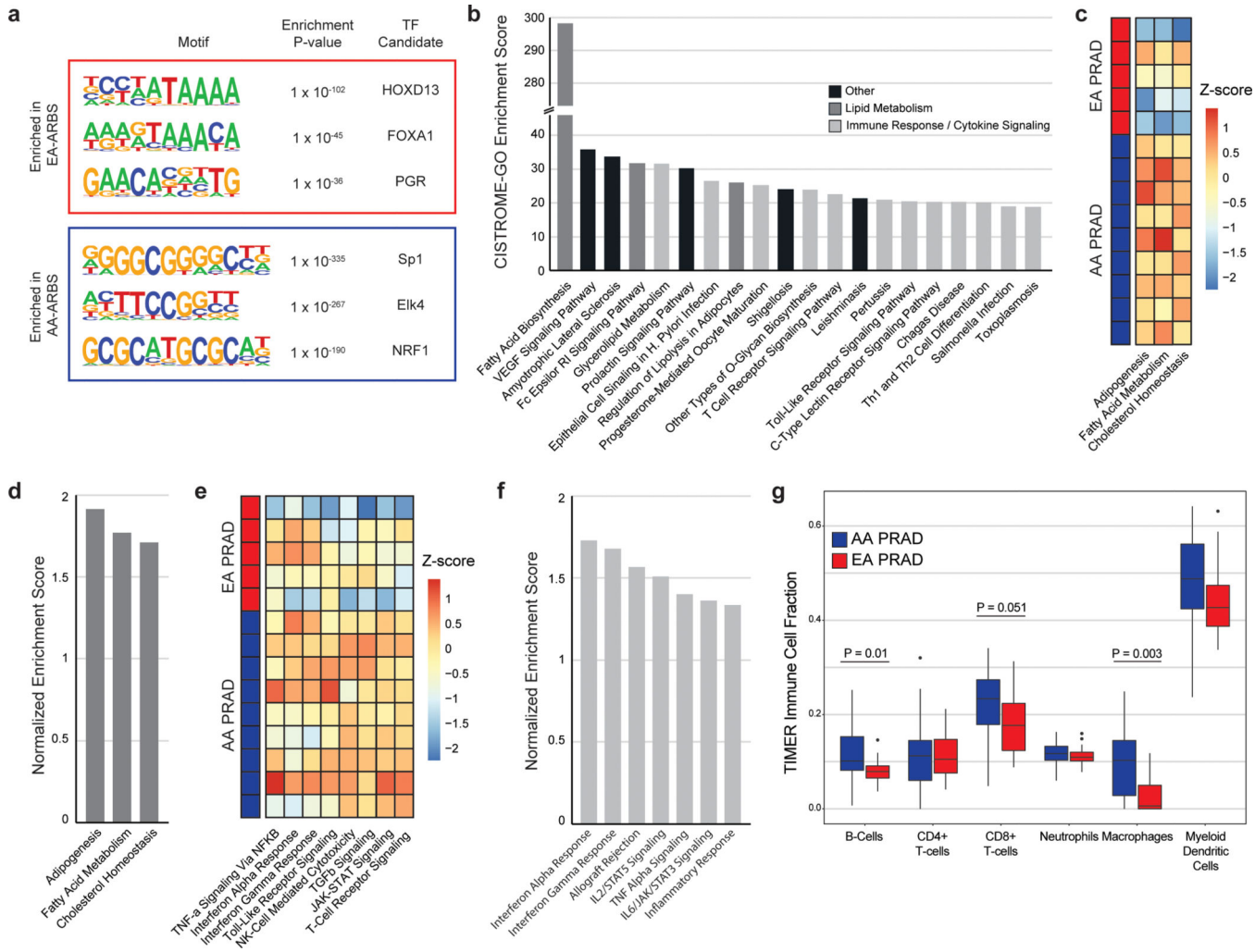

Figure 3.

The AR PCa cistrome associates with lipid metabolism, immune response, and cytokine signaling. **a)** Three most significantly enriched nucleotide motifs present in AA-ARBS and EA-ARBS by de novo motif analysis. **b)** Pathway enrichment of the AA-ARBS identified using CISTROME-GO.(23) AR binding intensity in each AA and EA prostate tumor for Hallmark lipid metabolism **(c)** and immune response and cytokine signaling **(e)** gene sets using ssGSEA analysis.(24) Differential expression analysis in our RNA-seq data identifies upregulation of Hallmark lipid metabolism **(d)** and immune response and cytokine signaling **(f)** gene sets in AA (n=30) versus EA (n=19) prostate tumors. **g)** Estimation of tumor infiltrate immune populations demonstrates greater signal for B-cells (P = 0.01) and macrophages (P = 0.003), and a trend towards CD8+ T-cells (P = 0.051) in AA versus EA PCa.(41)

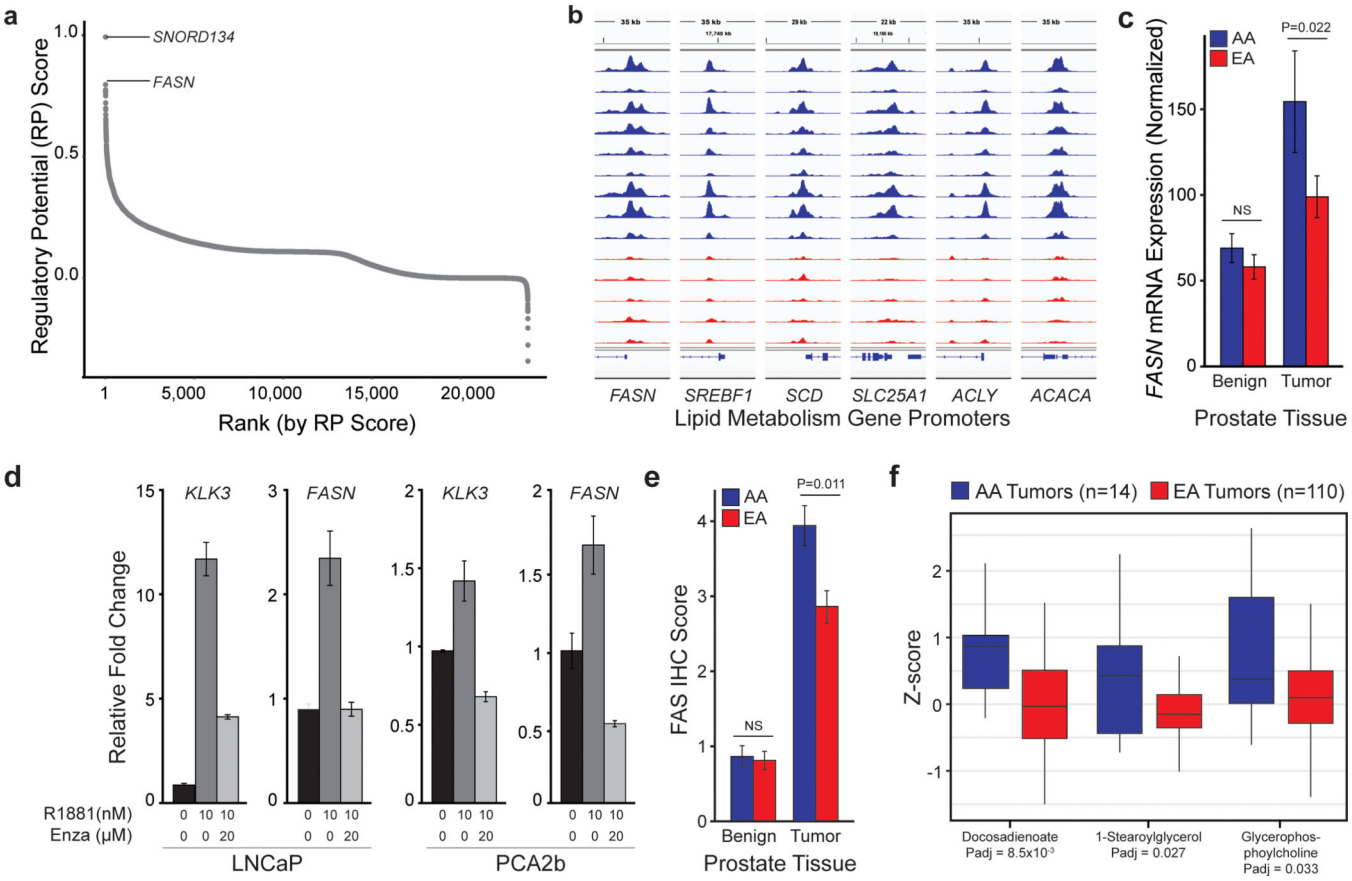

Figure 4.

AR binding associates with *FASN* and other lipid metabolism genes, which are regulated by AR *in vitro*. **a)** Gene-level regulatory potential (RP) score in the 16,678 AA-ARBS identifies *FASN* as the gene with the greatest difference in AR binding intensity in AA versus EA PCa.(23) **b)** AR binding intensity is greater in AA than EA prostate tumors at the *FASN* promoter, as well as several other genes that encode key lipid metabolism enzymes. Each track depicts ChIP-seq AR binding intensity in each sample. **c)** Normalized *FASN* mRNA expression in paired normal prostate tissue and PCa from 24 AA and 24 EA men. Error bars reflect the standard error. **d)** RNA expression for *FASN* and *KLK3* in LNCaP cells and PCA2b cells treated with vehicle, R1881 for 72 hours, or R1881 72 hours and enzalutamide for 48 hours. Expression values for cells treated with R1881 or R1881 plus enzalutamide are relative to vehicle-treated cells (black). Error bars reflect the standard error. **e)** FAS protein expression in 492 prostate tissue specimens from AA (102 tumor and 112 normal) and EA men (150 tumor and 128 normal) demonstrating significantly higher FAS expression in AA than EA prostate tumors. Error bars reflect the standard error. **f)** Metabolomic analysis of 94 lipids in 14 AA and 110 EA prostate tumors identified lipids and fatty acids present at significantly higher levels in AA prostate tumors. Box plots are displayed with a median center line, box range from the 25th to 75th percentile and whiskers extending to the most extreme observation within 1.5 times the interquartile range.

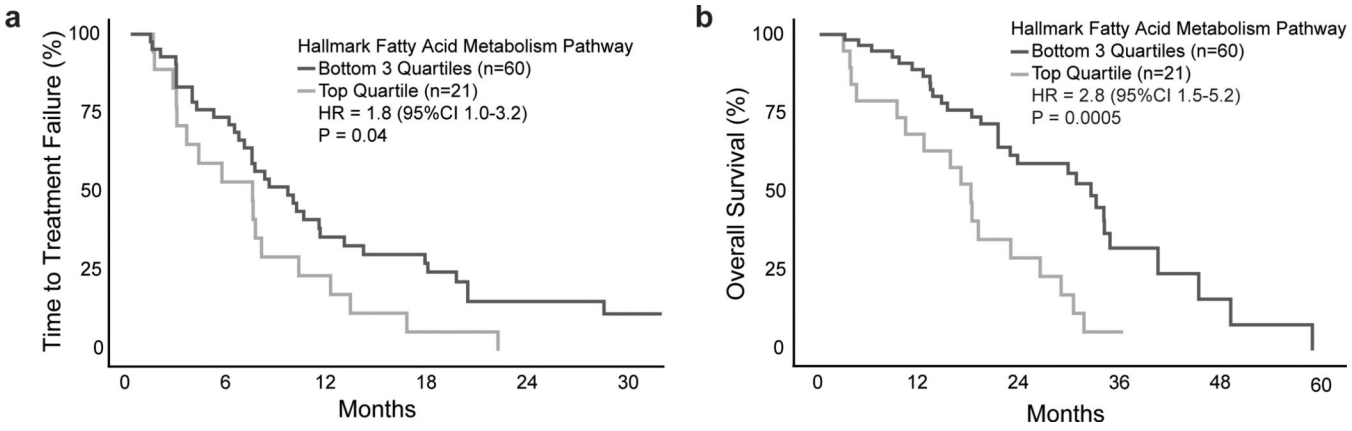

Figure 5.

Upregulated lipid metabolism is associated with worse prostate cancer outcomes. Kaplan-Meier survival curves for time to treatment failure **(a)** and overall survival **(b)** on abiraterone or enzalutamide for 81 men with metastatic castration-resistant PCa based on lipid metabolism activity.(36) Lipid metabolism scores were generated by applying ssGSEA to normalized RNA-seq data and extracting sample-level enrichment scores for the Hallmark Fatty Acid Metabolism gene set. Outcomes were compared between men in the top quartile versus the lower three quartiles based on ssGSEA enrichment scores.